INT. J. REMOTE SENSING, 2003, VOL. 24, NO. 8, 1765–1781

Taylor & Francis
Taylor & Francis Group

Fire and smoke observed from the Earth Observing System MODIS instrument—products, validation, and operational use

Y. J. KAUFMAN[1]*, C. ICHOKU[1,2], L. GIGLIO[2,3], S. KORONTZI[4,5], D. A. CHU[1,2], W. M. HAO[6], R.-R. LI[1,2] and C. O. JUSTICE[4,3]

[1]NASA/Goddard SFC, Laboratory for Atmospheres (913), Greenbelt MD 20771, USA
[2]Science Systems and Applications Inc, 10210 Greenbelt Road, Lanham, MD 20706, USA
[3]NASA/Goddard SFC, Laboratory for Terrestrial Physics (923), Greenbelt MD 20771, USA
[4]Department of Geography, University of Maryland, College Park, MD 20742, USA
[5]Department of Environmental Sciences, University of Virginia, Charlottesville, VA 22903, USA
[6]Rocky Mountain Research Station, Forest Service, USDA, Missoula, MT 59807, USA

Abstract. The Moderate Resolution Imaging Spectroradiometer (MODIS) sensor, launched on the National Aeronautics and Space Administration Terra satellite at the end of 1999, was designed with 36 spectral channels for a wide array of land, ocean, and atmospheric investigations. MODIS has a unique ability to observe fires, smoke, and burn scars globally. Its main fire detection channels saturate at high brightness temperatures: 500 K at 4 μm and 400 K at 11 μm, which can only be attained in rare circumstances at the 1 km fire detection spatial resolution. Thus, unlike other polar orbiting satellite sensors with similar thermal and spatial resolutions, but much lower saturation temperatures (e.g. Advanced Very High Resolution Radiometer and Along Track Scanning Radiometer), MODIS can distinguish between low intensity ground surface fires and high intensity crown forest fires. Smoke column concentration over land is for the first time being derived from the MODIS solar channels, extending from 0.41 μm to 2.1 μm. The smoke product has been provisionally validated both globally and regionally over southern Africa and central and south America. Burn scars are observed from MODIS even in the presence of smoke, using the 1.2 to 2.1 μm channels. MODIS burned area information is used to estimate pyrogenic emissions. A wide range of these fire and related products and validation are demonstrated for the wild fires that occurred in northwestern USA in Summer 2000. The MODIS rapid response system and direct broadcast capability is being developed to enable users to obtain and generate data in near real-time. It is expected that health and land management organizations will use these systems for monitoring the occurrence of fires and the dispersion of smoke within two to six hours after data acquisition.

*Corresponding author; e-mail: kaufman@climate.gsfc.nasa.gov

This paper was presented at the 3rd International Workshop of the Special Interest Group (SIG) on Forest Fires of the European Association of Remote Sensing Laboratories held in Paris in May 2001.

International Journal of Remote Sensing
ISSN 0143-1161 print/ISSN 1366-5901 online © 2003 Taylor & Francis Ltd
http://www.tandf.co.uk/journals
DOI: 10.1080/01431160210144741

1. Introduction

In December 1999, the National Aeronautics and Space Administration (NASA) launched the Moderate Resolution Imaging Spectrometer (MODIS) on the polar-orbiting Earth Observation System's (EOS) Terra spacecraft for global observations, with equator crossing times around 10:30 am and 10:30 pm local times. A second MODIS instrument was launched onboard the Aqua spacecraft on 4 May 2002, providing afternoon and night observations at 1:30 pm and 1:30 am. These four MODIS observations are being used to derive the daily fire and smoke distributions among other products. MODIS has special channels for global fire monitoring with 1 km resolution at 4 μm and 11 μm, with high saturation temperatures of about 500 K and 400 K, respectively (Kaufman *et al.* 1998 a). Seven of its spectral channels from 0.41 μm to 2.13 μm wavelength are being used to observe aerosol (including smoke) characteristics over land and ocean (Chu *et al.* 2001, Remer *et al.* 2001). MODIS data are used to monitor active fires, burn scars (Justice *et al.* 1996), vegetation type and condition, water vapour and clouds.

MODIS data are processed daily and archived by the NASA Distributed Active Archive Centers (DAAC) for the entire globe. Direct broadcasting data can be received in near real-time locally and can be used to generate fire and smoke products in close to real-time over an area of 4 million km^2 (with a swath width of 2330 km) for each receiving station. There are currently about two dozen MODIS direct broadcasting systems already in place around the world (http://rsd.gsfc.nasa.gov/eosdb/).

The interest in monitoring fires and smoke from space stems from the recognition that biomass burning is a major source of trace gases and aerosol particles, with significant ramifications for atmospheric chemistry, cloud properties, and radiation budgets (Crutzen *et al.* 1979, Crutzen and Andreae 1990, Kaufman *et al.* 1990, 1992, Kaufman and Nakajima 1993, Hao and Liu 1994, Skole *et al.* 1994, Kaufman and Fraser 1997) and, consequently, for climate (Penner *et al.* 1992, Dickinson 1993, Andreae *et al.* 1994, IPCC 1995). Fire is also a considerable and continuous factor in the ecology of savannas, boreal forests and tundra, and plays a major role in deforestation in tropical and sub-tropical regions. On a periodic basis, extensive fires also occur naturally in many temperate biomes such as forests, grasslands, and chaparral. Fire is an integral part of land use in many parts of the world, particularly in the tropics.

A methodology adopted by the Intergovernmental Panel on Climate Change (IPCC) to derive national emission estimates from fires is based on national annual inventories of fire extent and area burned. However, the quality of these national greenhouse gases inventories needs more vigorous evaluation. Other assessment approaches use operational remote sensing of fires from the Advanced Very High Resolution Radiometer (AVHRR) sensor aboard the National Oceanic and Atmospheric Administration's (NOAA) polar orbiting satellite, especially in the tropics (Setzer and Pereira 1991, Scholes *et al.* 1996) and boreal region (Li *et al.* 2000 a, b). Monitoring fires and smoke simultaneously by remote sensing was suggested by Kaufman *et al.* (1990). New approaches that incorporate remote sensing of burn scars left by fires are also emerging (Roy *et al.* 2002). The MODIS fire products are intended to be used together with fire products derived from the Geostationary Operational Environmental Satellites (GOES) (Prins and Menzel 1992, 1994, Prins *et al.* 1998), which can provide additional information on the daily cycle of fire activity, though at a lower resolution of 4 km. Other satellites also detect the presence of fires and can measure the smoke density or optical thickness. Data

from the Along Track Scanning Radiometer (ATSR) have been used to detect nighttime fires and aerosol products (Legg and Laumonier 1999, Veffkind *et al.* 2000). Data from the Tropical Rainfall Measuring Mission (TRMM) sensor are used to detect fires over the tropics and the mid-latitudes (Giglio *et al.* 2000). The Total Ozone Mapping Spectrometer (TOMS) ultraviolet data are used to detect thick elevated smoke and ozone (Herman *et al.* 1997).

The objective of this paper is to present the current status of MODIS remote sensing of fires and fire-related phenomena such as smoke and burned areas as well as their derivative products. It is a review paper aimed at assessing the performance of MODIS in these areas at the background of results of pre-launch feasibility studies. The versatile role of MODIS in fire science will be critically examined. Highlights of the MODIS fire algorithms and products are available on the MODIS Fire and Thermal Anomalies web site: http://modis-fire.gsfc.nasa.gov.

2. Background

The MODIS Fire Science Team (MFST) has developed algorithms that use thermal signatures to separate the fire signal from the background signal. Extensive evaluation of the MODIS algorithm prior to launch was undertaken using aircraft and satellite data from the Yellowstone wildland fire of 1988 and prescribed fires in the Smoke, Cloud, and Radiation (SCAR) aircraft and field experiments in California (SCAR-C) and Brazil (SCAR-B) (Kaufman *et al.* 1996, 1998 a, b). The data were used to establish the relationship between the fire thermal properties, the rate of biomass consumption and burn scar growth and the emissions of aerosol and trace gases from fires. The pre-launch experimental results will be briefly summarized in §2.1, to provide a background for later discussion of the fire products and post-launch validation results.

2.1. *Results of pre-launch experiments*

Figure 1 (after Kaufman *et al.* 1998 a) presents the main results of the SCAR-C experiment. Here, the thermal emission from a single fire was monitored from the ER-2 aircraft as a function of time. The NASA ER-2 aircraft flew the MODIS airborne simulator (MAS) to measure the fire thermal and mid-IR signature with a 50 m spatial resolution. The thermal radiation is computed from the observations at 1.6 μm, assuming that each pixel is a black body (the 3.9 μm channel saturated over the fire in this experiment). The rate of emission of smoke particulates is derived from MAS observations of smoke at 0.66 μm over the ocean a few kilometres downwind of the fire. There is very good agreement between the rate of emission of smoke particles and the rate of emission of the thermal energy from the fire. These two are also compared with the size of fires as detected by MAS at 4 μm as well as the Forest Service model predictions of the heat release and the total particulate mass for sizes smaller than 2.5 μm. The Forest Service model was derived from ground-based observations of the fuel load, ignition and consumption. It is very difficult to predict the fire emission and rate of burn within a factor of 2.

During the SCAR-B experiment in 1995, we also tested the MODIS fire methodology using MAS data flown on the ER-2. These data were used to observe the thermal properties and sizes of fires in the cerrado grassland and Amazon forests of Brazil and to simulate the performance of the MODIS 1 km resolution fire observations. Although some fires saturated the 50 m resolution MAS 3.9 μm channel, all the fires were well within the MODIS 1 km instrument saturation levels. Figure 2

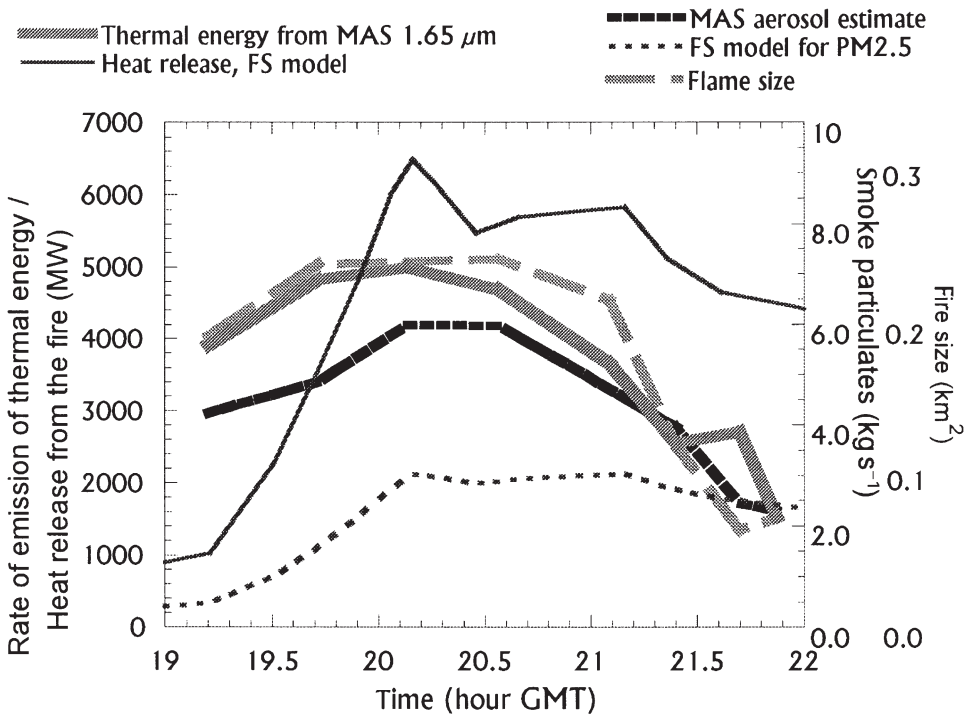

Figure 1. Relationship between the rate of emission of thermal radiative energy and smoke particulates from a prescribed fire in Oregon in 1994, based on MODIS Airborne Simulator (MAS) measurements aboard the ER-2 aircraft. The model predictions of the Forest Service (FS) for the heat release and for the total particulate mass for size under 2.5 μm are superimposed. Note the strong similarity between the time dependence of the rate of emission of radiative energy, the fire size and the rate of emission of smoke as obtained from the remote sensing data (after Kaufman *et al.* 1998 a).

(after Kaufman *et al.* 1998 b) shows the relationships obtained from the experiment. The MAS data used are for 11 September 1995 over a dense Cerrado region north of Pôrto Nacional. Each observation provided the fire thermal radiative energy (E_f) by using a composite of the radiance at 3.9 and 2.1 μm. The power law correlation between the integrated radiative energy and the change in burn scar (ΔS_f) is 97 per cent. The correlation between the burn scar change (ΔS_f) and the integrated fire size (Σ_f) is 86 per cent. This difference in the correlation shows that the fire radiative energy is four times better, as an indicator of the rate of biomass consumption, than only the fire size.

Analysis of MAS data over four sites, representing different ecosystems, shows that the fire sizes varied from single MAS pixels (50 m $\times$ 50 m) to over 1 km^2. At 1 km resolution, the MODIS instrument can observe only 30–40 per cent of these fires. However, the observed fires are mostly larger fires (flame covering more than 100 m^2) that are responsible for 80 per cent to nearly 100 per cent of the emitted radiative energy and therefore for 80 to 100 per cent of the rate of biomass burning in the region. The rate of emission of radiative energy from the fires was found to correlate very well with the formation of the burn scar from the fire (correlation coefficient = 0.97).

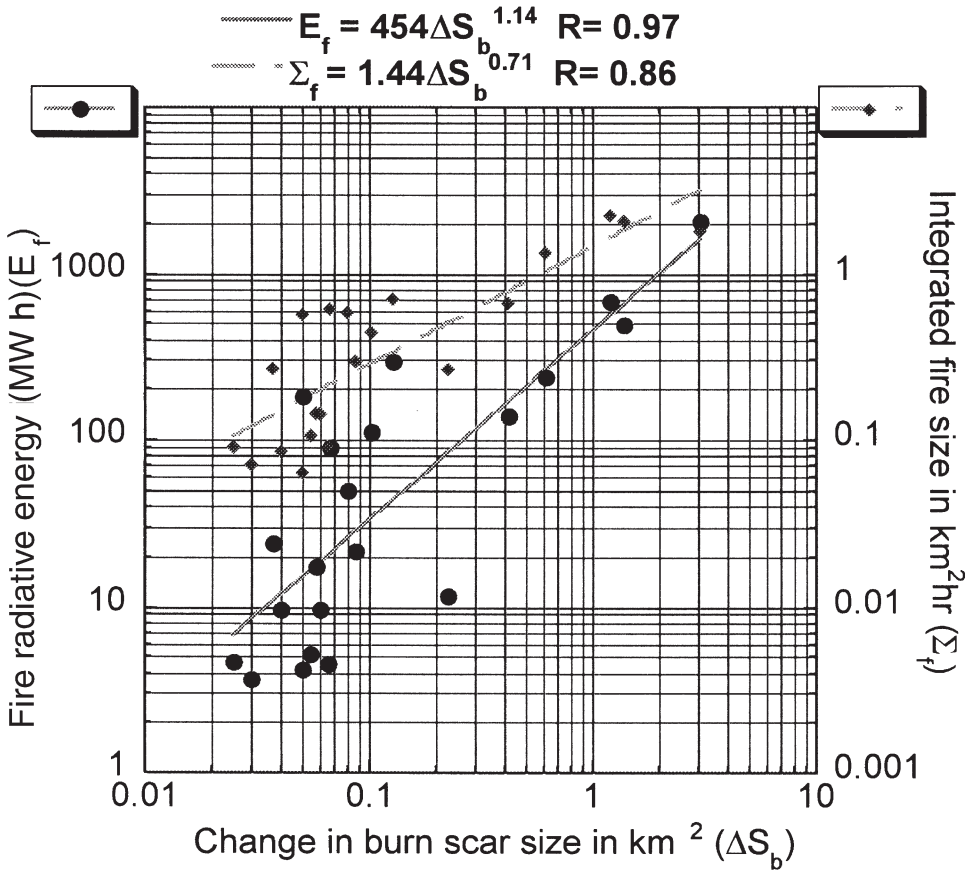

Figure 2. Results from MAS measurements of fires in northeast Brazil during the SCAR-B experiment. The MAS data are for 11 September 1995 over a dense Cerrado region north of Pôrto Nacional. The ER-2 flew over the same region and fires six times every 50 minutes. The integrated radiative energy (E_f) emitted from the fire between the first and last observation of the fire (left scale) and integrated fire size Σ_f (right scale) are plotted as a function of the increase in the burn scar ΔS_f between these observations (after Kaufman *et al.* 1998 b).

2.2. *MODIS fire products*

The MODIS active fire products are operationally generated and archived at 1 km spatial resolution (the Level 2 product). These are composited to produce the Level 3 daily and 8-day global products, both of which are also at 1 km resolution.

A new set of derivatives of the active fire product is currently under development. These derivative products will be summarized on a daily, weekly, and monthly basis over the entire globe on a grid of 1° spatial resolution, and with selected information at 10 km resolution. The parameters derived will include the fire occurrence and location, the rate of emission of thermal energy from the fire, a measure of the rate of biomass burning, and a rough estimate of the smoldering-to-flaming ratio. This information will be used to monitor the spatial and temporal distribution of fires in different ecosystems, to detect changes in fire distribution and identify new fire frontiers, and changes in the frequency of the fires or their relative strength. Given that these environmental factors are crucial in climate modelling, which can easily

assimilate such coarse (1°) resolution data, these active fire derivative products will be referred to as fire Climate Modelling Grid (CMG) products.

Aerosol parameters constitute another major set of fire related products currently being retrieved operationally from MODIS, including the aerosol optical thickness (AOT, representing the total column concentration), size parameters, and a characterization of the aerosol type. Fine aerosol particles, which include smoke, originate from biomass burning or from urban/industrial emissions, as opposed to coarse particles, which often consist of dust. Mixed state aerosols are also retrieved.

3. Generation of MODIS fire and aerosol products

Although the MODIS fire and aerosol algorithms were described in previous papers prior to launch (Kaufman *et al.* 1997, Tanre *et al.* 1997, Kaufman *et al.* 1998 a), for completeness in this paper, it is essential to understand the processes and status of the product generation. This section summarizes the characteristics of the fire and aerosol products described in this paper and the processes involved in their generation based on the use of real MODIS data.

3.1. *The active fire detection process*

Active fire detection is performed using the MODIS 4 and 11 μm channels (Kaufman *et al.* 1998 a). The MODIS instrument has two 4 μm channels, bands 21 and 22, both of which are used by the detection algorithm. Channel 21 saturates at $\sim$500 K, and channel 22 saturates at 335 K. Since channel 22 has lower noise and a smaller quantization error, it is used whenever possible. However, when channel 22 saturates or has missing data, the higher-range channel 21 is used instead. This selection takes place on a per-pixel basis. The 250 m near-infrared band (channel 2), averaged to 1 km resolution, is employed to identify reflective surfaces more likely to cause false alarms.

This algorithm identifies active fires using both absolute and relative detection criteria; in this sense it is a hybrid threshold/contextual algorithm (Justice and Dowty 1994). The absolute criteria are used primarily to identify the more intense and/or larger fires, while the relative criteria are intended to identify smaller fires by accounting for the natural variability in temperature and emissivity of the surface and reflection by sunlight. Sun-glint rejection is performed for all daytime observations, taking into consideration the satellite and sun geometry. Finally, a detection confidence estimate is provided to help users gauge the quality of individual fire pixels. A detailed description of the current algorithm is provided in Justice *et al.* (2002).

3.2. *The fire CMG product*

Fires generate smoke aerosols and gases, which are major contributors to atmospheric constituents. These constituents attenuate solar radiation directly through scattering and absorption. Also, they modify cloud microphysical properties, thereby influencing the way clouds attenuate solar radiation, a phenomenon known as the 'indirect aerosol effect'. Fire radiative energy can constitute an additional energy source on the atmospheric radiation budget. Furthermore, fires consume biomass, which is an important process within the biogeochemical cycles of carbon, nitrogen, and water. The resulting modification to the distribution of atmospheric constituents could have a major effect on the overall climate situation. Therefore, depending on its strength, distribution, and frequency, fire is a force to consider among other global climate change factors (Justice and Korontzi 2001). As such, fires should be

taken into serious consideration when modelling the climate and its dynamics. The fire CMG product is designed primarily to facilitate the incorporation of MODIS active fire products into climate models.

The fire CMG product is being developed on a 1-degree resolution global grid. The Level 2 active fire pixels (1 km resolution) are consolidated as described by Kaufman *et al.* (1998 a) before they are used to generate the CMG. Table 1 lists the parameters that will be included in the product. The first five parameters represent a summary of the spatial characteristics of the Level 2 (1 km resolution) active fire product within each grid cell of the CMG. They include the ratio of Level 2 pixels (out of the total number of pixels in each grid cell): (i) processed, (ii) containing fire, (iii) covering water bodies, or (iv) covered by clouds. All the foregoing parameters are expressed as a percentage. In addition, the total radiative energy generated within each grid cell is computed and expressed in MW (megawatts) as described in Kaufman *et al.* (1998 a). This first group of parameters is also generated on a spatial grid of 10 km resolution, corresponding to the resolution of the MODIS Level 2 aerosol product, to facilitate the direct correlation of the fire and aerosol products.

The second group of parameters in the CMG product comprises statistics of the actual fire physical properties within each grid cell. Only the active fire pixels are considered. These are binned in accordance with the value of the pixel brightness temperatures in the main fire detection channel, which is the 4 μm wavelength channel (denoted by T_4). Typical T_4 values for fires range between 315 K and 500 K. This range will be divided into 10 classes approximately with equal class intervals. The fire pixels within each grid cell are assigned into their corresponding T_4 histogram

Table 1. Contents of the fire Climate Modelling Grid (CMG) product at 1×1 degree spatial resolution. Items 1–5 have one value per grid cell regardless of fire temperature, while for items 6–13 the brightness temperatures of the fire pixels at approximately 4 μm wavelength are binned into several class intervals, and the parameters are derived for each class, resulting in as many layers of each parameter as the number of classes. Items 1–5 are also computed at 10×10 km spatial resolution.

Serial no.	Product description	Number of layers	Units
1	Ratio of processed-to-total pixel count within the grid cell	1	%
2	Ratio of fire-to-total pixel count within the grid cell	1	%
3	Ratio of water-to-total pixel count within the grid cell	1	%
4	Ratio of cloud-to-total pixel count within the grid cell	1	%
5	Total fire radiative energy within the grid cell	1	MW
6	Number of fire pixels per class (based on T_4 bins)	N_c	
7	Fire radiative energy per class	N_c	MW
8	Mean value of T_4 per class	N_c	K
9	Mean value of T_{11} per class	N_c	K
10	Mean value of $T_4 - T_{11}$ per class	N_c	K
11	Mean value of $T_4 - \mu T_{4bg}$ per class	N_c	K
12	Mean value of $T_{11} - \mu T_{11bg}$ per class	N_c	K
13	Ratio of smoldering-to-total fire per class	N_c	%

T_4 = pixel brightness temperature value at approximately 4 μm.
μT_{4bg} = background mean brightness temperature value at approximately 4 μm.
T_{11} = pixel brightness temperature value at approximately 11 μm.
μT_{11bg} = background mean brightness temperature value at approximately 11 μm.
N_c = number of classes (i.e. bins of T_4).

classes. For each grid cell, each of the parameters numbered 6 to 13 in table 1 is computed, separately for each class. These histogram classes are represented as separate layers of each individual parameter.

3.3. *The MODIS smoke aerosol*

The MODIS aerosol algorithm employs the physical principles of attenuation of solar radiation by aerosols to infer aerosol characteristics such as the aerosol optical thickness (AOT) and particle size parameters. Because of the difference in the optical properties of land and oceanic surfaces, different procedures are used to retrieve aerosols over land and over ocean. Over land surfaces, AOT is computed at 0.47 and 0.66 μm wavelengths, which are then interpolated to derive AOT at 0.55 μm, whereas over the ocean, AOT retrieval is accomplished at seven wavelengths: 0.47, 0.55, 0.66, 0.87, 1.2, 1.6, and 2.1 μm. The generation methodology and validation of the MODIS aerosol products are described in Chu *et al.* (2002) and Remer *et al.* (2002). Although AOT is derived for all aerosols integrally, it is possible to distinguish smoke aerosols from others (such as dust and sulphates) based on their size differences and absorption. Smoke optical thickness of up to 3 can be derived from the MODIS data. The optical thickness is defined as the absolute logarithm of the vertical transmisson of sunlight through the smoke aerosol. Under average solar illumination conditions, an optical thickness of up to 3 corresponds to a reduction of the direct sunlight reaching the ground by a factor of 20 to 100.

4. Evaluation of MODIS fire/smoke products

Validation of the active fire products is difficult due to the sporadic and heterogeneous occurrence of fires. Studies from intensive field campaigns in southern Africa (SAFARI-2000) and Brazil (LBA-2000) and fires in northwestern USA (the 2000 fire season) are ongoing to evaluate the product accuracy for fire detection and characterization. However, we have an indication of the likely validity of the MODIS smoke product from pre-launch experiments (Chu *et al.* 1998) and post-launch evaluation (Chu *et al.* 2002) using measurements from the AErosol RObotic NETwork (AERONET) of ground-based radiometers (Holben *et al.* 1998). A few examples of MODIS smoke and fire data, selected from the first year of MODIS operation, are described for three regions of the world.

4.1. *Southern African fires*

A large intensive field campaign known as the SAFARI-2000 was conducted in southern Africa during August and September 2000. The campaign, implemented within the framework of an international science initiative with NASA participation, was aimed at studying and addressing the linkages between land–atmosphere processes and the relationship of biogenic, pyrogenic or anthropogenic emissions and the consequences of their deposition to the functioning of the biogeophysical and biogeochemical systems of southern Africa (http://safari.gecp.virginia.edu/). However, one of the main practical applications of the experiment has been to validate the data products acquired by most of the EOS remote-sensing instruments, including MODIS.

On different days during SAFARI-2000, several prescribed fires were set at various locations within the southern African region, and the fire characteristics and emissions were measured with numerous ground-based and airborne instruments and sensors, concurrently with satellite acquisitions. Unfortunately, MODIS encountered

some technical problems, which caused data acquisition to be skipped during the initial part of the campaign in the first half of August 2000. However, it recovered quickly and acquired data during the remainder of the SAFARI-2000 period.

Figure 3(*a*) shows a global composite at 1° spatial resolution of the MODIS Level 3 aerosol optical thickness (AOT) product at 0.55 μm wavelength for September 2000. The magnified southern African region shows heavy concentrations of smoke aerosols generated mostly by wildland fires and prescribed fires during the SAFARI-2000 experiment. The smoke transport over the Atlantic Ocean is clearly visible. Histograms of the AOT derived from the southern African data are shown in figure 3(*b*) separately for land and ocean. MODIS Level 2 aerosol products, from which the level 3 product was derived, and which have a spatial resolution of 10 km have been validated using ground based AOT acquisitions from AERONET sunphotometers/sky radiometers (Holben *et al.* 1998). The validation data comprise spatial statistics of MODIS AOT data within 50 km × 50 km boxes centred over each AERONET station and temporal statistics of the sunphotometer data spanning the period 30 minutes before and 30 minutes after the MODIS overpass (Ichoku *et al.* 2002). Scatter plots of the MODIS spatial mean AOT against the AERONET temporal mean AOT at 0.47 μm (blue) and 0.66 μm (red) wavelengths, generated from data acquired concurrently by the two instruments in southern Africa during SAFARI-2000, showed excellent linear correlation at both wavelengths. At the 0.47 μm waveband, the regression equation was $y=0.90x-0.02$, with correlation coefficient $r=0.93$, while at 0.66 μm they were $y=0.92x-0.03$ and $r=0.92$ (Chu *et al.* 2001).

4.2. *Central/South American fires*

Figure 4 is a typical example of the MODIS analysis of the smoke optical thickness from a single fire, in this case from Mexico in Central America (19 April 2000). As indicated earlier, smoke is analysed over land and ocean with different algorithms because of the differences between the reflective properties of land and ocean surfaces. However, it is interesting to note that similar aerosol retrieval results are obtained on both sides of the seashore.

MODIS spatial mean AOT retrieved over several locations in South America during the period July–September 2000 has been validated against corresponding temporal mean of ground-based AERONET Sun-photometer AOT. Scatter plots show excellent linear correlation between the parameters from the two instruments. The regression equations (and corresponding correlation coefficients) were $y=1.02x+0.014$ ($r=0.98$) and $y=0.86x-0.012$ ($r=0.94$) at 0.47 μm and 0.66 μm respectively (Chu *et al.* 2002). The correlation coefficients are even slightly better than those of the southern Africa (above).

4.3. *North American fires*

In Summer 2000 severe wildland fires burned unprecedented areas of forested land in Montana and Idaho, among other states in the USA. In figure 5 we examine the fires in Montana, using the MODIS data acquired on 23 August 2000. A composite image of the detected fire locations (red dots) superimposed on a land surface colour image (from the blue, green and red visible channels) is shown (figure 5(*a*)). It visually validates the fire locations as the locations from which smoke is emitted. The MODIS derived smoke optical thickness is shown in the adjoining panel (figure 5(*b*)). The area delimited by the rectangle in figure 5(*a*) is represented with enlargement for a closer view of the fires and smoke (figure 5(*c*)), burn scars

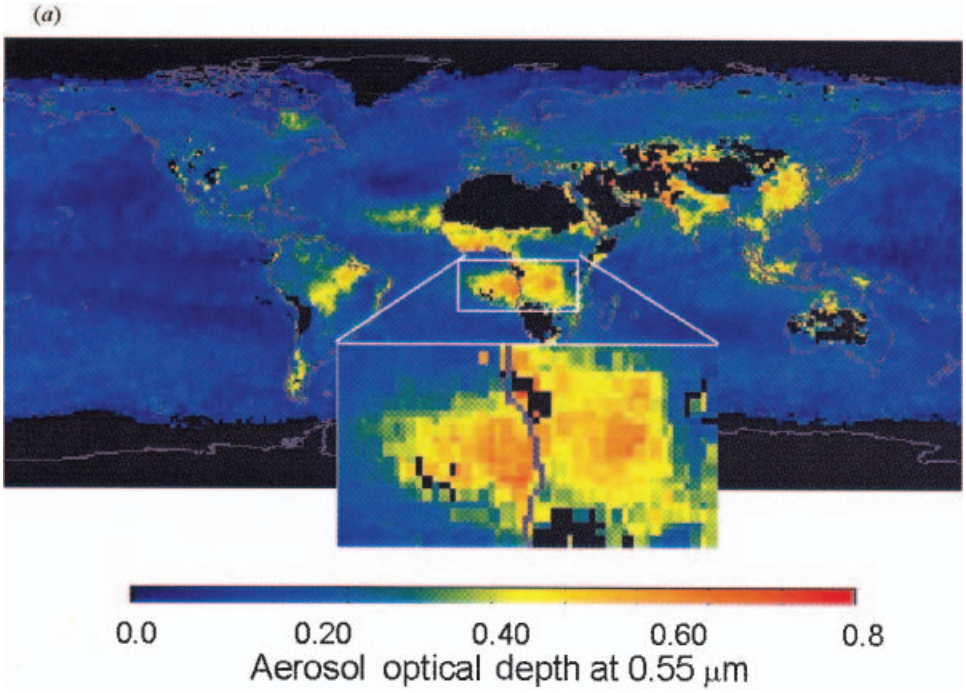

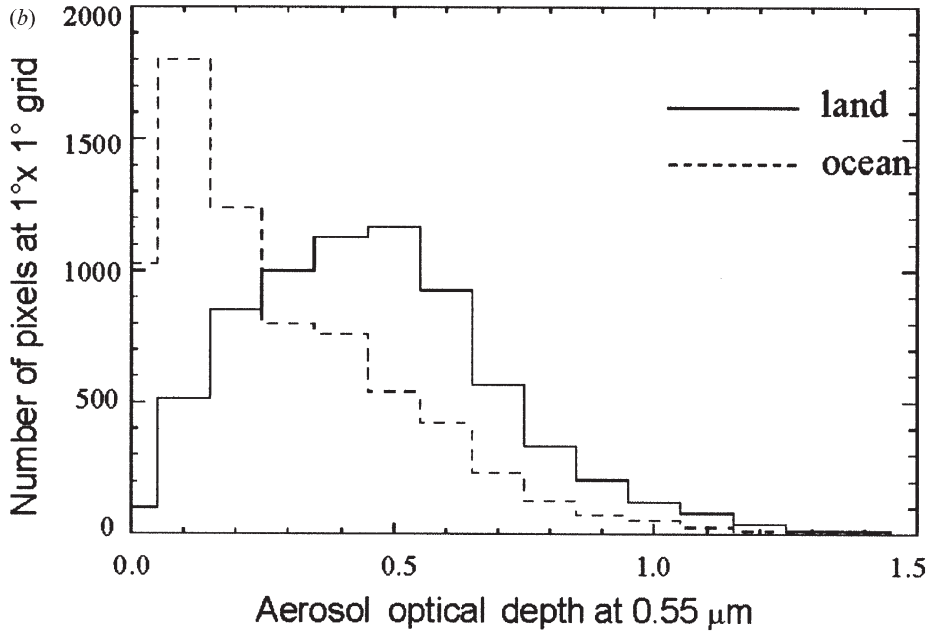

Figure 3. (*a*) Global composite of MODIS aerosol optical thickness (AOT) product at 0.55 μm wavelength for September 2000 at 1° spatial resolution. The magnified southern African region shows a heavy concentration of smoke aerosols generated mostly by the prescribed and other wildland fires during the SAFARI-2000 experiment. The smoke transport over the Atlantic Ocean is clearly visible. (*b*) Histograms of the AOT plotted from the southern African data separately for land and ocean.

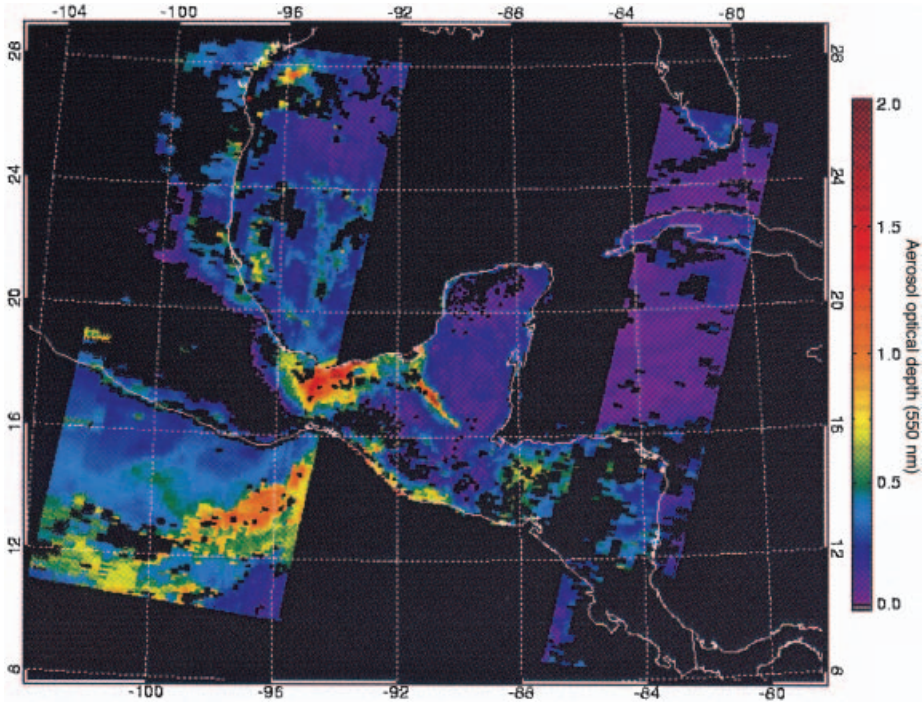

Figure 4. Smoke from a fire in Central America detected by MODIS 2 months after the beginning of operations (19 April 2000). The scale on the right gives the smoke optical thickness (detected over land or ocean). Note the continuity of the smoke from land to ocean despite different assumptions and calculations of the ocean and land algorithms. The black regions are either clouds that were screened out or the glint region over the ocean.

(figure 5(*d*)), and fire apparent temperatures (figure 5(*e*)). The burn scars (figure 5(*d*)) are observed through the smoke using a colour composite based on longer wavelengths (1.2, 1.65 and 2.1 μm), where smoke particles are transparent. Also MODIS 4 μm channel brightness temperatures show correspondence between the fire locations and the high temperature pixels (figure 5(*e*)).

Ground-based visual validation of the fire strength was conducted by the US Forest Service a few days after the fire. In figure 6 we 'zoom' into the MODIS fire data to observe a single large fire in Montana. The temperature of the fire pixels varies across the fire. Part of the variation can be due to the triangular response of MODIS, whereby a fire in a given location can be observed in two adjacent pixels along the scan line (across the orbital swath). However, ground based photographs show the correspondence between the MODIS pixels and the post-fire vegetation density, which can be used to assess the fire severity qualitatively. This qualitatively estimated fire severity or rate of biomass consumption relates well to the strength of the fire detected by MODIS (represented by the fire brightness temperatures at 4 μm). The central red dot (390 K) corresponds to extreme severity of this crown fire that burned up to the top branches of the trees. The yellow dots (350 K) correspond to only spotty burns of the crowns of the trees with most of the branches remaining intact. The green dots (330 K) correspond to spotty fire or moderate intensity understory fires. Note that previous satellite sensors used to detect fires, such as

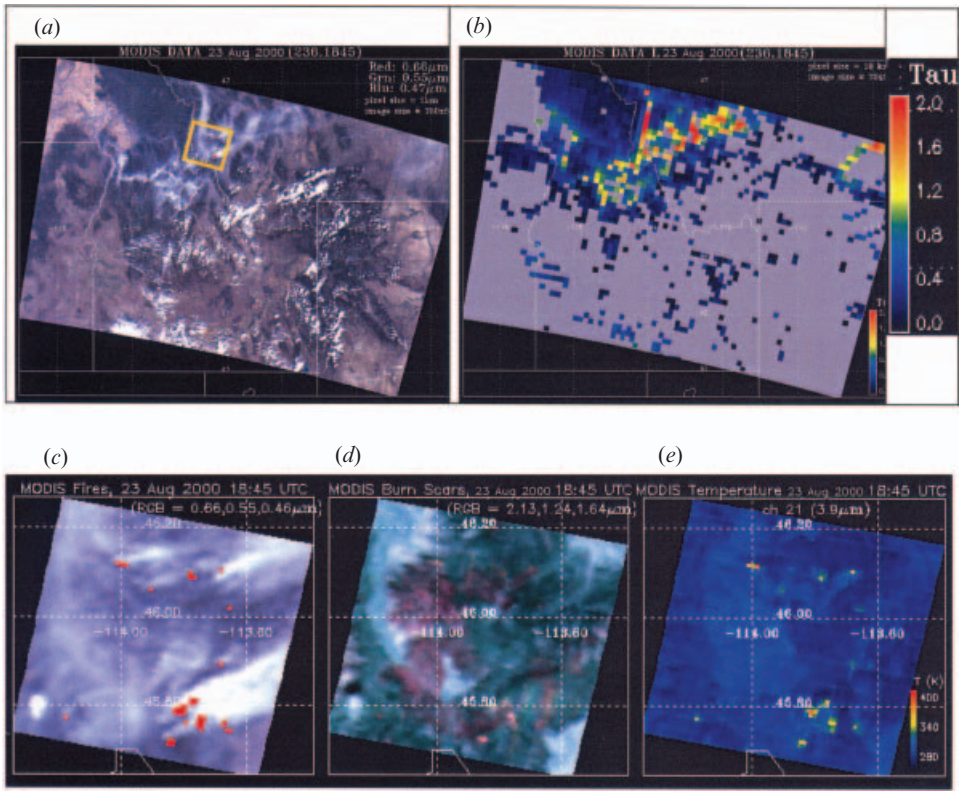

Figure 5. MODIS image of wildfires in Montana and Idaho on 23 August 2000. Top set of images: (*a*) colour composite of the MODIS blue, green and red channels, showing the smoke from the fires, with red dots representing fire pixels detected with the MODIS 4 μm channel at 1 km spatial resolution. Burn scars are dark. (*b*) The smoke optical thickness derived with the MODIS aerosol algorithm at 10 km spatial resolution. The colour bar on the right shows the AOT levels. Closer views of the area delineated by the gold rectangle on (*a*) show: (*c*) fire pixels and smoke, (*d*) colour composite with the 1.2, 1.65 and 2.13 μm channels (green, red and blue respectively) revealing the dark burn scars more prominently, (*e*) fire pixel brightness temperatures at 4 μm.

the AVHRR, ATSR, DMSP, and GOES, cannot distinguish between these cases due to their low saturation brightness temperature (around 325–335 K) in their fire detection channel.

In addition to the above qualitative validation of the active fires, we determined the extent and atmospheric impacts of these wildfires in an area around the borders of Montana/Idaho using the MODIS burned area information. The 5 September 2000 MODIS image (figure 7(*a*)) was subsetted from the MODIS, Level 2G, 1 km Surface Reflectance Product. The band combination of 6, 5, 2 was used for red, green and blue respectively, for the visualization. The middle infrared band 5 has the property of enhancing burn scars, shown here as dark brown areas. Because fast re-growth is not an issue in large forest fires, as opposed to savanna ecosystems for example, this image is believed to be representative of the total burned area from the beginning of the fires in Summer 2000 until 5 September 2000, the date of the image. This MODIS image shows a burned area of 506 100 ha, which is very close

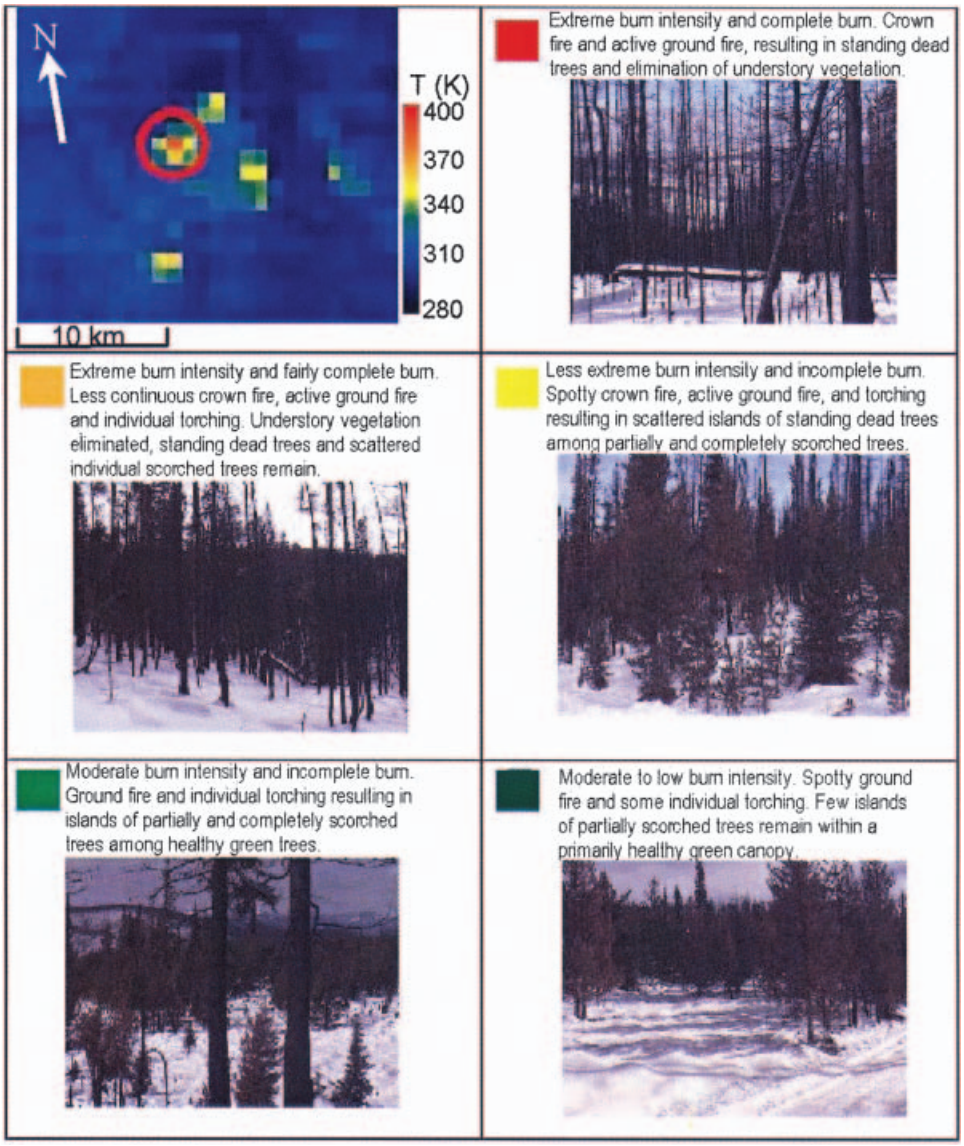

Figure 6. Fire intensity observations in relation to the 4 μm brightness temperatures from MODIS (top left) of the large fires at the lower right part of figure 5 (*a*), (*b*), (*c*). The colour scale shows the fire apparent temperatures at 4 μm. Photographs of the area burned and explanations of the findings are given for each of the fire pixels in the encircled area. The stronger the fire temperature observed by MODIS, the higher the concentration of the biomass fuel consumed.

to the burned area of 425 000 ha determined from ground survey by the Forest Service. This accounted for about 14 per cent of the 2000 annual total area burned in the USA (source: National Interagency Fire Center (NIFC), http://www.nifc.gov). A comparison of historical statistical data from NIFC indicates that the total annual area burned in 2000 was twice the average area burned in the period 1990–1999 and the highest in the last 40 years. The total carbon dioxide (CO_2), carbon monoxide

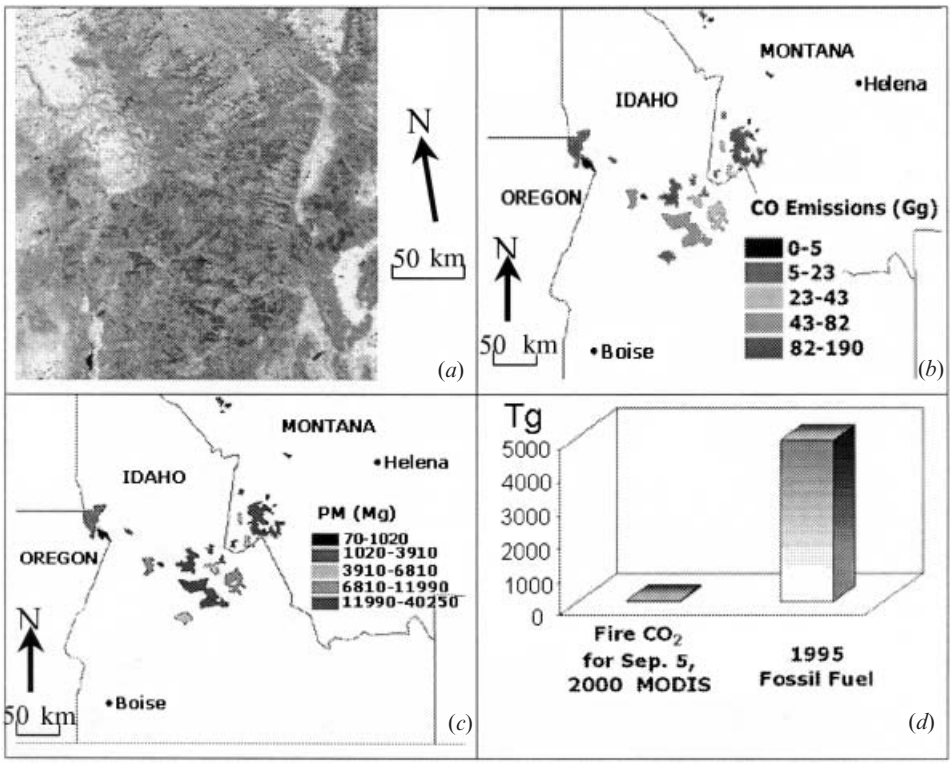

Figure 7. Computation of fire emissions over western USA: (*a*) MODIS burned area composite (channel assignments: red = 6, blue = 5, green = 2) of the Idaho/Montana border region, 5 September 2000. Burn scars are dark brown; (*b*) CO emissions magnitude and spatial distribution from the 2000 Idaho/Montana wildfires leading up to that data; (*c*) PM emissions magnitude and spatial distribution for the same location and period; (*d*) Comparison of CO_2 emissions from the 2000 Idaho/Montana wildfires with the 1995 fossil fuel CO_2 emissions reported by EPA.

(CO), and total particulate matter (PM) emissions from each burn scar were obtained by multiplying the MODIS area burned with the typical biomass fuel loadings from the National Fire Danger Rating System (NFDRS) fuel model (Deeming *et al.* 1977, Burgan 1988), a combustion efficiency of 0.85, typical for forest fires (Hardy *et al.* 1992) and emission factors for CO_2 CO and PM from Ward and Hardy (1991). The CO and PM distributions are shown in figures 7(*b*) and 7(*c*), respectively. These fires produced a total of 31 026 Gg of CO_2, 760 Gg of CO and 159 000 Mg of PM. Despite the devastating fires and the resulting emissions, fossil fuel emissions are by far the prevailing source for CO_2 emissions in the USA (EPA 1997) (figure 7(*d*)). Using this analysis approach, MODIS burned area information will greatly improve the accuracy of current fire emissions modelling at the regional level.

5. Discussions and conclusions

Fires and smoke are fascinating scientific elements. However, fire and the toxic pollutants it generates can be dangerous and have to be closely monitored. The MODIS instrument, launched at the end of 1999 was designed with a unique ability to observe a suite of fire related products: active fires, smoke and burn scars.

Preliminary results show that MODIS is capable of distinguishing different fire intensities based on brightness temperature differences, although more comparisons with ground-based observations are needed. The solar channels of MODIS extending from 0.4 to 2.1 μm are excellent to derive the smoke column concentration over land. This product is already well-validated based on comparisons with ground-based AERONET sun photometer measurements. Burn scars can be observed from the MODIS mid-infrared channels ranging from 1.2 to 2.1 μm even in the presence of smoke, which are transparent at that wavelength range. The MODIS burned area information is starting to be used in pyrogenic emissions modelling.

The new MODIS instrument capability of measuring fires, smoke and burn scars, and the ability to broadcast the data directly and to freely disseminate the information in near real-time, makes it ideal for regional monitoring of fire activity and the spread of smoke and other emissions. We tested this capability for northwestern USA using expedited MODIS data, before the direct broadcast system became available. Fire and smoke images, such as the one shown in figure 5 were generated and transmitted electronically within 14 hours to the Forest Service North Rockies Coordination Center in Missoula, Montana. They were then used together with other information to monitor the regional fire situation. Based on this experience the Forest Service is installing a MODIS direct broadcast receiving system, and will analyse fire characteristics and smoke dispersion within a few hours of data acquisition. It is expected that health and land management organizations will use this technology to obtain data for monitoring the occurrence of fires and the spread of smoke and other emissions.

References

Andreae, M. O., Fishman, J., Garstang, M., Goldammer, J. G., Justice, C. O., Levine, J. S., Scholes, R. J., Stocks, B. J., and Thompson, A. M., 1994, Biomass burning in the global environment: first results from the IGAC/BIBEX Field Campaign STARE/TRACE-A/SAFARI-92. In *Global Atmospheric-Biospheric Chemistry*, edited by R. G. Prinn (New York: Plenum), pp. 83–101.

Burgan, R. E., 1988, Revisions to the 1978 nation fire-danger rating system. US Department of Agriculture, Forest Service Research Paper SE-273.

Chu, D. A., Kaufman, Y. J., Ichoku, C., Remer, L. A., Tanre, D., and Holben, B. N., 2002, Validation of MODIS aerosol optical depth retrieval over land. *Geophysical Research Letters*, **29**(12).

Chu, D. A., Kaufman, Y. J., Remer, L. A., and Holben, B. N., 1998, Remote Sensing of Smoke from MODIS Airborne Simulator During SCAR-B Experiment. *Journal of Geophysical Research*, **103**, 31 979–31 988.

Crutzen, P. J., and Andreae, M. O., 1990, Biomass burning in the tropics: impact on atmospheric chemistry and biogeochemical cycles. *Science*, **250**, 1669–1678.

Crutzen, P. J., Heidt, L. E., Krasnec, J. P., Pollock, W. H., and Seiler, W., 1979, Biomass burning as a source of atmospheric gases: CO, H_2, N_2O, NO, CH_3Cl, and COS. *Nature*, **282**, 253–256.

Deeming, J. E., Burgan, R. E., and Cohen, J. D., 1977, The national fire-danger ration system—1978. US Department of Agriculture, Forest Service General Technical Report INT-39.

Dickinson, R. E., 1993, Effect of fires on global radiation budget through aerosol and cloud properties. In *Fire in the Environment: The ecological, atmospheric, and climatic importance of vegetation fires*, edited by P. J. Crutzen and J. G. Goldammer (New York: John Wiley & Sons), pp. 107–122.

EPA (US Environmental Protection Agency), 1997, National air quality and emissions trends report, 1995. EPA, Office of Air Quality Planning and Standards, Triangle Park, North Carolina, USA.

Giglio, L., Kendall, J. D., and Tucker, C. J., 2000, Remote sensing of fires with the TRMM VIRS. *International Journal of Remote Sensing*, **21**, 203–207.

Hao, W. M., and Liu, M.-H., 1994, Spatial and temporal distribution of tropical biomass burning. *Global Biogeochemical Cycles*, **8**, 495–503.

Hardy, C. C., Ward, D. E., and Einfield, W., 1992, PM2.5 Emissions from a major wildfire using a GIS: rectification of airborne measurements. *Air and Waste Management Association Annual Meeting Pacific Northwest International Section, Bellevue, Washington, 11–13 November 1992* (Pittsburgh, PA: Air and Waste Management Association), pp. 1–12.

Herman, J. R., Barthia, P. K., Torres, O., Hsu, C., Seftor, C., and Celarier, E., 1997, Global distribution of UV absorbing aerosol from Nimbus 7/TOMS data. *Journal of Geophysical Research*, **102**, 16 911–16 922.

Holben, B. N., Eck, T. F., Slutsker, I., Tanré, D., Buis, J. P., Setzer, A., Vermote, E., Reagan, J. A., Kaufman, Y. J., Nakajima, T., Lavenu, F., Jankowiak, I., and Smirnov, A., 1998, AERONET-A federated instrument network and data archive for aerosol characterization. *Remote Sensing of Environment*, **66**, 1–16.

Ichoku, C., Chu, D. A., Mattoo, S., Kaufman, Y. J., Remer, L. A., Tanré, D., Slutsker, I., and Holben, B., 2002, A spatio-temporal approach for global validation and analysis of MODIS aerosol products. *Geophysical Research Letters*, **29**(12).

IPCC (Intergovernmental Panel on Climate Change), 1995, *Climate Change 1994*, edited by J. T. Houghton, L. G. Meira Filhno, J. B. Hoesung Lee, B. A. Callander, E. Haites, N. Harris and K. Maskell (Cambridge: Cambridge University Press).

Justice, C. O., and Dowty, P. (editors), 1994, *IGBP-DIS satellite fire detection algorithm workshop technical report*. IGBP-DIS Working Paper 9, NASA/GSFC, Greenbelt, MD, February 1993.

Justice, C. O., and Korontzi, S., 2001, A review of the status of satellite fire monitoring and the requirements for global environmental change research. In *Global and Regional Vegetation Fire Monitoring from Space: Planning and coordinated international effort*, edited by F. Ahern, J. Goldammer and C. O. Justice (The Hague: SPB Academic Publishing), pp. 1–18.

Justice, C. O., Giglio, L., Roy, D., Korontzi, S., Owens, J., Descloitres, J., Alleaume, S., Petitecolin, F., and Kaufman, Y., 2002, The MODIS Fire Products: algorithm, preliminary validation and utilization, *Remote Sensing of Environment*, in press.

Justice, C. O., Kendall, J. D., Dowty, P. R., and Scholes, R. J., 1996, Satellite remote sensing of fires during the SAFARI campaign using NOAA advanced very high radiometer data. *Journal of Geophysical Research*, **101**, 23 851–23 863.

Kaufman, Y. J., and Fraser, R. S., 1997, The effect of smoke particles on clouds and climate forcing. *Science*, **277**, 1636–1639.

Kaufman, Y. J., and Nakajima, T., 1993, Effect of Amazon smoke on cloud microphysics and albedo-analysis from satellite imagery. *Journal of Applied Meteorology*, **32**, 729–744.

Kaufman, Y. J., Justice, C. O., Flynn, L. P., Kendall, J. D., Prins, E. M., Giglio, L., Ward, D. E., Menzel, W. P., and Setzer, A. W., 1998 a, Potential global fire monitoring from EOS-MODIS. *Journal of Geophysical Research*, **103**, 32 215–32 238.

Kaufman, Y. J., Kleidman, R. G., and King, M. D., 1998 b, SCAR-B fires in the tropics: properties and their remote sensing from EOS-MODIS. *Journal of Geophysical Research*, **103**, 31 955–31 969.

Kaufman, Y. J., Remer, L. A., Ottmar, R. D., Ward, D. E., Li, R.-R., Kleidman, R., Fraser, R. S., Flynn, L., McDougal, D., and Shelton, G., 1996, Relationship between remotely sensed fire intensity and rate of emission of smoke: SCAR-C experiment. In *Global Biomass Burning*, edited by J. Levin (Cambridge, MA: The MIT press), pp. 685–696.

Kaufman, Y. J., Setzer, A., Ward, D., Tanré, D., Holben, B. N., Menzel, P., Pereira, M. C., and Rasmussen, R., 1992, Biomass Burning Airborne and Spaceborne Experiment in the Amazonas (BASE-A). *Journal of Geophysical Research*, **97**, 14 581–14 599.

Kaufman, Y. J., Tanré, D., Remer, L. A., Vermote, E., Chu, A., and Holben, B. N., 1997, Operational remote sensing of tropospheric aerosol over land from EOS moderate resolution imaging spectrometer. *Journal of Geophysical Research*, **102**, 17 051–17 067.

Kaufman, Y. J., Tucker, C. J., and Fung, I., 1990, Remote sensing of biomass burning in the tropics. *Journal of Geophysical Research*, **95**, 9927–9939.

Legg, C. A., and Laumonier, Y., 1999, Fires in Indonesia, 1997: a remote sensing perspective. *AMBIO*, **28**, 479–485.

Li, Z., Nadon, S., and Cihlar, J., 2000 a, Satellite-based detection of Canadian boreal forest fires: development and application of the algorithm. *International Journal of Remote Sensing*, **21**, 3057–3069.

Li, Z., Nadon, S., Cihlar, J., and Stocks, B., 2000 b, Satellite-based mapping of Canadian boreal forest fires: evaluation and comparison of algorithms. *International Journal of Remote Sensing*, **21**, 3071–3082.

Penner, J. E., Dickenson, R. E., and O'Neill, C. A., 1992, Effects of aerosol from biomass burning on the global radiation budget. *Science*, **256**, 1432–1434.

Prins, E. M., and Menzel, W. P., 1992, Geostationary satellite detection of biomass burning in South America. *International Journal of Remote Sensing*, **13**, 2783–2799.

Prins, E. M., and Menzel, W. P., 1994, Trends in South American biomass burning detected with the GOES Visible Infrared Spin Scan Radiometer Atmospheric Sounder from 1983 to 1991. *Journal of Geophysical Research*, **99**, 16 719–16 735.

Prins, E. M., Feltz, J. M., Menzel, W. P., and Ward, D. E., 1998, An overview of GOES-8 diurnal fire and smoke results for SCAR-B and 1995 fire season in South America. *Journal of Geophysical Research*, **103**, 31 821–31 835.

Remer, L. A., Tanré, D., Kaufman, Y. J., Ichoku, C., Mattoo, S., Levy, R., Chu, D. A., Holben, B. N., Dubovik, O., Ahmad, Z., Smirnov, A., Martins, J. V., and Li, R.-R., 2002, Validation of MODIS Aerosol Retrieval Over Ocean. *Geophysical Research Letters*, **29**(12).

Roy, D. P., Lewis, P. E., and Justice, C. O., 2002, Burned area mapping using multi-temporal moderate spatial resolution data—a bi-directional reflectance model-based expectation approach. *Remote Sensing of Environment*, in press.

Scholes, R. J., Ward, D. E., and Justice, C. O., 1996, Emissions of trace gases and aerosol particles due to vegetation burning in southern hemisphere Africa. *Journal of Geophysical Research*, **101**, 23 677–23 682.

Setzer, A. W., and Pereira, M. C., 1991, Amazonia biomass burnings in 1987 and an estimate of their tropospheric emissions. Ambio, **20**, 19–22.

Skole, D., Moore, B., and Chomentowski, W., 1994, Spatial analysis of land cover change and carbon flux associated with biomass burning in Brazil 1970–1980. In *Climate Biosphere Interaction*, edited by R. Zepp (New York: John Wiley and Sons), pp. 161–202.

Tanré, D., Kaufman, Y. J., Herman, M., and Mattoo, S., 1997, Remote sensing of aerosol properties over oceans using the MODIS/EOS spectral radiances. *Journal of Geophysical Research*, **102**, 16 971–16 988.

Veefkind, J. P., de Leeuw, G., Stammes, P., and Koelemeijer, R. B. A., 2000, Regional distribution of aerosol over land, derived from ATSR-2 and GOME. *Remote Sensing of Environment*, **74**, 377–386.

Ward, D. E., and Hardy, C. C., 1991, Smoke emissions from wildland fires. *Environmental Information*, **17**, 117–134.